

U.S. DEPARTMENT OF COMMERCE  
NATIONAL OCEANIC AND ATMOSPHERIC ADMINISTRATION  
NATIONAL WEATHER SERVICE  
SYSTEMS DEVELOPMENT OFFICE  
TECHNIQUES DEVELOPMENT LABORATORY

TDL OFFICE NOTE 83- 8

IMPROVED 6-, 12-, 18-, AND 24-H EXTRATROPICAL STORM SURGE  
FORECAST GUIDANCE FOR BOSTON, MASS.; NEW YORK, N.Y.;  
NORFOLK, VA.; AND CHARLESTON, S.C.

William S. Richardson and Craig S. Gilman

June 1983

IMPROVED 6-, 12-, 18-, AND 24-H EXTRATROPICAL STORM SURGE  
FORECAST GUIDANCE FOR BOSTON, MASS.; NEW YORK, N.Y.;  
NORFOLK, VA.; AND CHARLESTON, S.C.

William S. Richardson and Craig S. Gilman

1. INTRODUCTION

As more people and businesses move to the ocean front, the potential for serious damage resulting from extratropical storm surges increases. Along the United States' east coast the development of coastal communities and businesses has increased the need for accurate and timely storm surge forecast guidance.

The meteorologically generated storm surge (measured water level minus astronomical tide) is primarily caused by wind stress on the water surface. This surge, which is modified by nearshore bathymetry and the shoreline, is superimposed on the astronomical tide. When significant storm surges and associated wave action occur at the same time as high astronomical tides, serious flooding and beach erosion may occur.

2. BACKGROUND

The Techniques Development Laboratory (TDL) has developed automated extratropical storm surge forecast guidance for 12 tide gage locations (Portland, Maine; Boston, Mass.; Newport, R.I.; Stamford, Conn.; Willets Point, N.Y.; New York, N.Y.; Atlantic City, N.J.; Breakwater Harbor, Del.; Baltimore, Md.; Norfolk, Va.; Avon, N.C.; and Charleston, S.C.) along the east coast (National Weather Service, 1978). For each location (see Fig. 1), separate equations were derived with a multiple regression screening program (Pore et al., 1974). The regression program was used to correlate observed storm surge heights with analyzed sea-level pressures at 6-Level Primitive Equation (6LPE) model grid points.

Forecasts for the 12 tide gage locations are made by interpolating sea-level pressure forecasts of the Limited-area Fine Mesh (LFM) model to 6LPE grid points. These interpolated values are the predictors in the storm surge forecast equations. Storm surge forecasts at 6-h intervals (Fig. 2) are made twice each day to 48 hours.

In the very near future, observed storm surge heights at a number of east coast tide gage locations will become part of the National Meteorological Center's (NMC's) data base. Since this data base will be accessible to the automated storm surge forecast system, observed surge heights could be used as predictors in the storm surge forecast equations. In the short term, storm surge observations should be very good predictors of future surge heights.

This paper discusses the derivation of 6-, 12-, 18-, and 24-h forecast equations for Boston, Mass.; New York, N.Y.; Norfolk, Va.; and Charleston, S.C. These new equations use storm surge observations (measured water levels minus astronomical tides) in addition to sea-level pressures to forecast

surge heights. An evaluation of surge heights computed by these new equations is also presented.

### 3. DERIVATION

The new equations were derived with a multiple regression screening program. This regression program was used to correlate predictand data (measured surge heights) with observed predictors. This approach, where predictand data are correlated with observed predictors is called "perfect prog" in contrast to the Model Output Statistics (MOS) approach where predictand data are correlated with forecasts from a model. Screening for predictors was stopped when a predictor reduced the variance of the predictand less than 1 percent.

#### A. Predictand

The predictand, storm surge height, is a meteorologically-generated water level fluctuation. Storm surge heights at 0100, 0700, 1300, and 1900 EST were calculated by subtracting the astronomical tide heights from water levels measured by National Ocean Service (NOS) tide gages. From these calculated heights, we selected storm surge events. Each event, which began and ended with observed surge heights near zero, contained at least one observed height with a magnitude equal to or greater than 2 feet. Development samples varied in size from 53 storm surge events (597 6-h heights) at New York to 22 events (288 6-h heights) at Charleston. All storm surge events occurred from November through April and varied in length from 1 to 7 days.

#### B. Predictors

For each height, we offered the regression program analyzed sea-level pressures at 6-h intervals at 75 NMC grid points (Fig. 3) with time lags of 0, 6, 12, 18, and 24 hours. Also offered as predictors were the observed surge heights with 6-, 12-, 18-, and 24-h lags. Heights with lags greater than 24 hours were not considered as predictors because the correlation fell off rapidly after that time. We did not offer stability predictors (differences between and ratios of air and water temperature, and harmonics of an annual cycle) since these predictors were not selected in an earlier rederivation of the Charleston storm surge equation (Richardson and Boggio, 1980).

#### C. New Equations

The first predictor selected in the derivation of the 6-h equations for New York, Norfolk, and Charleston was, as expected, the observed surge height at the respective gage with a 6-h lag. However, the selection of predictors in the derivation of the Boston equation was unexpected. The observed surge height with a 6-h lag was not selected. Instead, the observed surge with a 12-h lag was selected as the fifth predictor. This unexpected selection of predictors may be due to the fact that surge heights which occur 12 hours apart are in nearly the same phase of the semidiurnal astronomical tide cycle. Surge heights which are 6 and 18 hours apart may occur in completely different phases of a tidal cycle. This semidiurnal relationship (surge heights 12 and 24 hours apart) may capture some of the non-linear

interactions between the astronomical tide and storm surge. These interactions are probably more pronounced at locations such as Boston where the tide range is large (9.5 feet).

For the 12-h equations, the first predictor selected for Norfolk was the observed storm surge height with a 12-h lag. The observed storm surge height with this lag was selected as the second predictor for Charleston and the third predictor for New York.

The observed surge height with an 18-h lag was selected as a predictor in the Norfolk 18-h equation. However, the observed surges with 18-h lags were not selected in the derivation of the Boston, New York, and Charleston equations. Surge heights with 24-h lags were selected instead. At Norfolk, the observed surge with a lag of 24 hours was selected as a predictor in the 24-h equation.

New equations are shown in the appendix. All constants and coefficients in all equations have been inflated. This inflation procedure partially corrects for underforecasting magnitudes of peak surge heights by multiplying surge heights by the reciprocal of the correlation coefficient which was calculated with the development sample. The average value of inflation factors is approximately 1.2. This same inflation procedure is used to produce the operational surge forecast guidance.

#### 4. EVALUATION

Storm surge heights specified (computed with analyzed, not forecast, sea-level pressures) by the new equations and the operational equations were evaluated in two ways. First, verification scores were computed and evaluated for independent events for each location. Second, comparisons of observed and specified surges were made for eight significant storm surge events.

##### A. Verification Scores

Table 1 shows the dates of independent events which were used in the evaluation. Tables 2 through 5 show the verification scores (correlation coefficient, RMSE, and weighted RMSE) associated with independent data for Boston, New York, Norfolk, and Charleston. The weighted RMSE (WRMSE), a new verification score, is calculated in the same manner as the RMSE when the magnitude of the observed surge height is 1 foot or less. For heights with magnitudes greater than 1 foot, the error (observed minus specified) is weighted by multiplying the error by the observed surge. The mathematical expression for WRMSE is:

$$\sum_{i=1}^n \left( \frac{[(O_i - S_i) W_i]^2}{n} \right)^{1/2},$$

where

n = number of observations in the surge event,

$O_i$  = i-th observed surge height,

$S_i$  = i-th specified surge height, and

$W_i$  = i-th weight, where  $W_i = 1$  if  $|O_i| \leq 1$ , or  $W_i = O_i$  (numerical value without units) if  $|O_i| > 1$ .

This statistic gives a heavier weight to an error that occurs when the magnitude of the surge is greater than 1 foot. Errors associated with high surge heights are more critical and are therefore given more weight.

Scores in the upper part of the tables are based on all independent data. The scores shown in the lower part of the tables were computed from peak (magnitude of measured surge equaled or exceeded 1.5 feet) data; 15 percent of the Boston data, 24 percent of the New York and Norfolk data, and 8 percent of Charleston data were in the peak data category.

The upper part of Table 2 shows the verification scores for Boston for all data. The 12- and 24-h equations are listed under the headings BOS12 and BOS24 respectively. The correlation coefficients associated with the new equations are only slightly larger than the correlation coefficient associated with the operational equation. Keep in mind that only one operational equation is used to make forecasts for all projections. Verification statistics for 6- and 12-h persistence are shown under the headings 6h and 12h. The RMSE's associated with the new equations are a little lower than the RMSE for the operational equation. For the 12-h equation, the WRMSE is a little lower than the error associated with the operational equation. However, WRMSE's associated with the 24-h and operational equations are nearly equal. Persistence at 12 hours is not as good a predictor as persistence at 6 hours. All of the above comparisons are valid for peak data, in the lower half of Table 2.

New York's verification scores for all data (top half of Table 3) and peak data (lower half of Table 3) show that the scores for the new equations are much better than the scores associated with the operational equation. The correlation coefficient associated with the 6-h equation, for all data, is 0.11 larger than the correlation coefficient for the operational equation. For all data, persistence at 6 hours beats the operational equation. The RMSE's and WRMSE's associated with the new equations are lower than those for the operational equation. Peak data statistics show a similar trend.

The verification scores for all data at Norfolk (top half of Table 4) are much more impressive than the scores for Boston and New York. The correlation coefficient was raised from 0.80 to 0.91 by including the storm surge height with a 12-h lag as a predictor. At the same time, the RMSE was reduced by almost 0.2 feet, while the WRMSE was lowered by 0.36 feet. The lower portion of Table 4, verification scores for peak data, shows that the correlation coefficients associated with the new equations are larger than those for the operational equation. The RMSE's and WRMSE's associated with the new 6-, 12-, and 18-h equations are much lower than those for the operational equation.

The verification scores associated with the new equations for Charleston for all data (top part of Table 5) are really eye catching. The correlation coefficient associated with the 12-h equation is 0.2 larger than that for the operational equation. Both 6- and 12-h persistence beat the operational equation. The RMSE and WRMSE are reduced by 0.2 feet. Notice that the correlation coefficient associated with the 12-h equation is larger than that for the 6-h equation. This may be due to the earlier discussed semidiurnal relationship between surge heights 12 hours apart. For all data, the



correlation coefficients associated with 6- and 12-h persistence are about the same. While the correlation coefficients associated with the new equations for peak data are not as impressive, the one for the 12-h equation is about one-half as large as the one for with the operational equation.

#### B. Significant Storm Surge Events

In addition to the statistics shown in Tables 2, 3, 4, and 5, we have also included discussions of eight independent storm surge events. Events were chosen by selecting the two events at each location with the highest observed storm surge height. Meteorological settings, measured surge heights, and heights specified by the 12-h equation and the operational equation are shown for each event. The inflated surge heights specified by the 12-h equation and the operational equation are plotted at 6-h intervals while solid lines connect hourly measured surge heights. Inflated surge heights specified by the 12-h equation are denoted by dots while inflated heights specified by the operational equation are shown as squares. The WRMSE's associated with the 12-h equation and the operational equation are given for each independent event. Dates are placed at 1200 EST. Discussions of the two Boston events are followed by discussions of two events for New York, Norfolk, and Charleston.

The first Boston event was caused by a storm which occurred in February 1972. On February 18 a low pressure system, centered over the Great Lakes, had a frontal system extending southward into the Gulf of Mexico. See Fig. 4. By 1300 EST, a closed low had developed over Georgia. Further development occurred and the storm moved rapidly toward the north-northeast, to a position just north of Cape Cod at 0100 EST on the 20th. The upper graph of Fig. 5 shows that the surge heights specified by the 12-h equation are in better agreement with the observed surge heights except for the peak surge. The WRMSE is approximately the same for each of the two equations.

Event number two resulted when a record-breaking storm occurred in early February 1978. This storm which formed off the South Carolina coast during the evening of February 5 (Fig. 6), intensified as it moved up the east coast. Cape Cod reported winds of 92 mph. Maximum surges occurred on February 6 and 7 (lower graph of Fig. 5). The surge heights specified by the 12-h equation are in better agreement (lower WRMSE) with the observed surge heights than the heights specified by the operational equation.

Storm surges during November 23-27, 1950 and November 4-8, 1953 are the two events presented for New York. The November 1950 storm was considered by some to be the worst storm on record for the eastern United States (Bristol, 1951). This storm caused record-breaking tides all along the northern east coast. Fig. 7 shows the sea-level pressure pattern associated with this event. The upper graph in Fig. 8 shows that the new 12-h equation specified the surge more accurately except for the peak values. For this reason the WRMSE associated with the 12-h equation is slightly larger than the WRMSE associated with the operational equation.

The storm associated with the November 1953 event caused strong onshore winds at many coastal locations. Fig. 9 contains 12-h surface pressure

charts from 0130 EST November 6 through 0130 EST November 8. At 0130 EST November 6, the low was located just off the Georgia-Florida coast. It progressed to the Cape Hatteras area by 1330 EST on the 6th, and to the Delaware area by 0130 EST on the 7th. The pressure gradient resulting from the low pressure of the storm and the high located over the Great Lakes area caused extremely high winds north of the storm center. The graph (lower graph of Fig. 8) for this event shows that the 12-h equation specified the surge much more accurately than the operational equation. This is also shown by the much lower (1.19 feet lower) WRMSE.

The two surge events discussed for Norfolk occurred during November 5-8, 1953 and April 25-29, 1978. The graph in the upper portion of Fig. 10 (November 1953) shows that the operational equation specified the peak surge more accurately than the 12-h equation. However, the graph associated with the April event (lower graph in Fig. 10) shows the opposite. The April storm deepened as it moved up the coast (Fig. 11). Maximum surges occurred at Norfolk on the 26th and 27th. Water levels remained well above normal through the 28th as the mature storm moved slowly northeastward. For the entire storm event, the surge heights specified by the 12-h equation are in much better agreement with the observed surge heights than the heights specified by the operational equation. This is also reflected in the much lower WRMSE, 0.96 feet for the 12-h equation compared to 2.03 feet for the operational equation.

While the November 1950 storm occurred near the time of spring tides and caused record-breaking tides from Maryland to New York, it caused only low water levels at Charleston. Fig. 7 (sea-level pressure patterns from November 24-26, 1950) shows that the general wind flow along the South Carolina coast is offshore by 0130 EST November 25. Approximately 9 hours after this time, Charleston experienced about a 3-ft negative surge (upper portion of Fig. 12). The surges specified by the 12-h equation and the operational equation are also negative. However, the surge specified by the 12-h equation is in better agreement with the measured peak negative surge than the surge specified by the operational equation. The measured surge and the surge specified by the 12-h equation remained negative for about 2 days while the surge computed by the operational equation returned to zero after 1 day. The WRMSE is about 1 foot lower for the 12-h equation.

In contrast to the November 1950 event, the December 1971 event was associated with a positive surge at Charleston. This event began when a low pressure system developed in the Gulf of Mexico on December 2, 1971 (Fig. 13). The system deepened and moved in a northeasterly direction, and was located off the South Carolina coast by the evening of December 3. The peak surge which occurred during the evening of December 3 is specified to be positive by both equations (lower graph of Fig. 12). The primary peak surge is specified more accurately by the operational equation. However, the secondary peak, which occurred during the early morning hours of the 4th, is specified more accurately by the 12-h equation. The WRMSE slightly favors the operational equation.

## 5. CONCLUSIONS

The statistical evaluation clearly shows that the surge heights specified by the new equations are significantly more accurate at New York, Norfolk,

and Charleston than heights specified by the operational equations. Verification scores associated with the new Boston equations are only slightly better than scores associated with the operational equation. Evaluations of storm surge graphs, with the WRMSE statistic, indicate the new equations specified the storm surge heights much more accurately than the operational equations for one of the two storm surge events at each location. The surge heights associated with the four remaining events were specified with approximately the same degree of accuracy by the new and operational equations, except for the peak surge heights which were specified a little more accurately by the operational equations. Verification scores and subjective evaluation of the eight surge events indicate that the new equations are better than the operational equations.

When storm surge observations at Boston, New York, Norfolk, and Charleston, become a part of the NMC data base, we suggest that:

- (1) The 6- and 12-h forecasts for Boston be made with the new 12-h equation. The 18- and 24-h forecasts be made with the new 24-h equation.
- (2) For New York, forecasts be made the same as (1), except the 6-h forecast be made with the new 6-h equation.
- (3) At Norfolk, the 6-, 12-, 18-, and 24-h forecasts be made with the new 6-, 12-, 18-, and 24-h Norfolk equations, respectively.
- (4) The new Charleston 12-h equation be used to make the 6- and 12-h forecasts for Charleston. Forecasts for 18 and 24 hours be made with the new 24-h equation.
- (5) Observed storm surge observations at the time of initial data (0000 or 1200 GMT) at Boston, New York, Norfolk, and Charleston be transmitted in place of the calculated surge heights.
- (6) Storm surge forecasts for 30, 36, 42, and 48 hours continue to be made with the operational equations.

We are investigating new variables which can be used to predict storm surges at Willets Point, N. Y. Experiments with persistence and astronomical tide heights did not improve surge forecasts for this location.

#### ACKNOWLEDGMENTS

We thank Art Pore and Kurt Hess for their helpful suggestions. We also thank Cindy Boggio for plotting the storm surge graphs. A special thanks to NOS for furnishing water level measurements.

#### REFERENCES

- Bristor, C. L., 1951: The great storm of November 1950. Weatherwise, 4, 10-16.



National Weather Service, 1978: Extratropical storm surge forecasts for the United States east coast. NWS Technical Proceedings Bulletin No. 226, National Oceanic and Atmospheric Administration, U.S. Department of Commerce, 5 pp.

Pore, N. A., W. S. Richardson, and H. P. Perrotti, 1974: Forecasting extratropical storm surges for the northeast coast of the United States. NOAA Technical Memorandum NWS TDL-50, National Oceanic and Atmospheric Administration, U.S. Department of Commerce, 70 pp.

Richardson, W. S., and C. L. Boggio, 1980: A new extratropical storm surge forecast equation for Charleston, South Carolina. TDL Office Note 80-7, National Weather Service, NOAA, U.S. Department of Commerce, 10 pp.

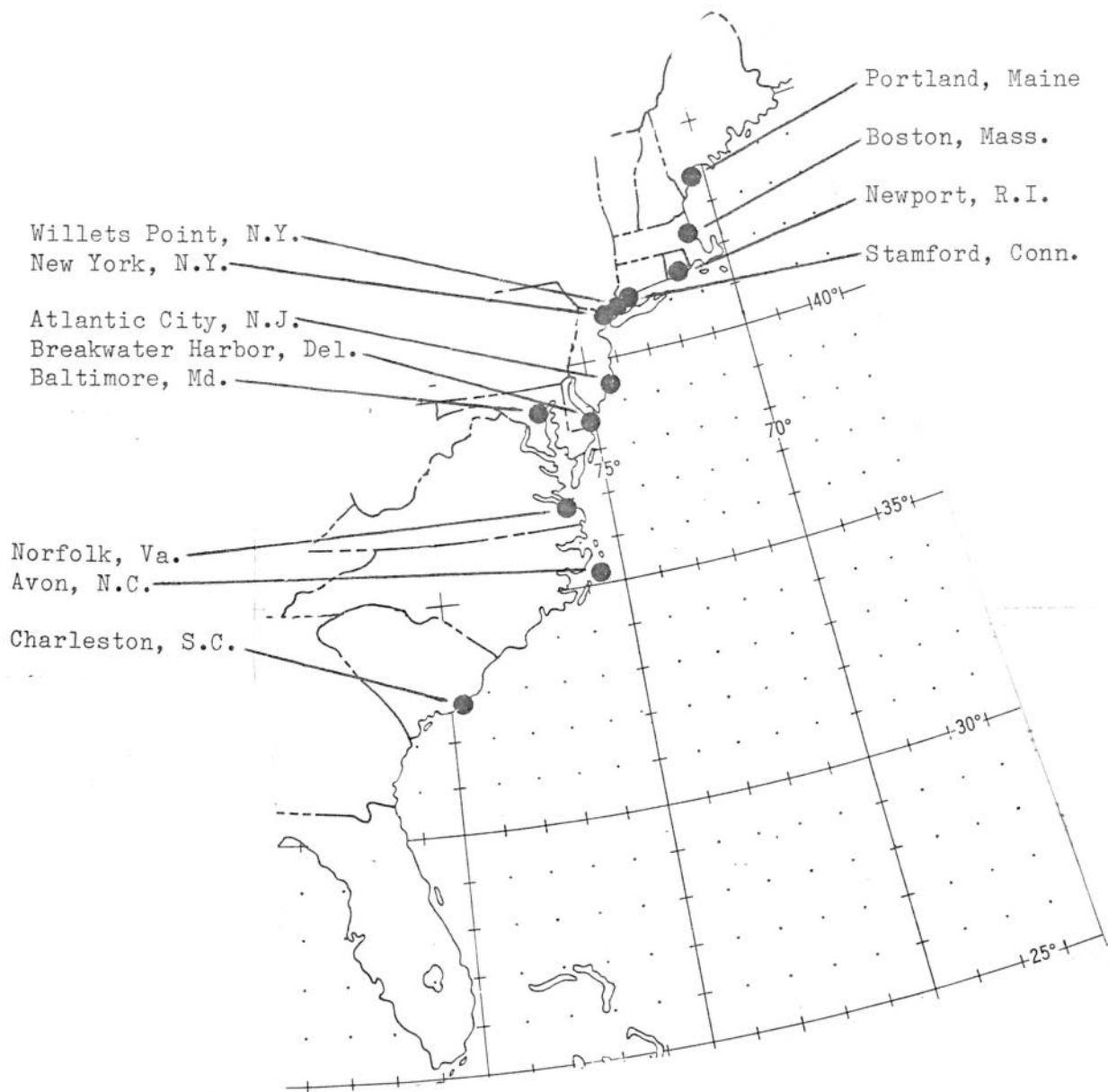


Figure 1. The 12 east coast locations for which automated extratropical storm surge forecasts are made.

FZUS3 KWBC 090000

STORM SURGE FCST FEET (INVALID FOR TROPICAL STORMS)

	00Z	06Z	12Z	18Z	00Z	06Z	12Z	18Z	00Z
PWM	0.1	0.6	0.9	1.5	1.6	1.8	1.6	1.4	1.0
BOS	-0.0	0.7	1.2	1.7	2.0	2.1	1.9	1.6	1.2
NWP	0.4	1.2	1.4	2.0	2.0	1.9	1.7	1.5	1.3
SFD	1.8	2.6	3.5	3.9	3.8	3.6	2.9	2.2	1.3
LGA	0.3	1.3	1.8	2.4	1.9	1.9	1.5	1.3	0.8
NYC	0.8	1.6	2.0	2.5	2.4	2.0	1.3	1.0	0.6
ACY	0.8	1.4	1.7	2.1	2.2	2.0	1.7	1.4	1.1
BWH	0.8	1.3	1.5	2.0	2.0	1.7	1.4	0.9	0.8
BAL	-0.0	0.2	0.4	0.2	-0.4	-1.0	-1.5	-1.4	-0.8
ORF	0.3	0.2	0.9	0.9	1.1	1.2	1.3	0.8	0.5
AVN	0.2	1.0	1.5	1.0	0.5	0.3	0.2	0.2	0.2
CHS	0.2	0.1	-0.6	-0.8	-1.3	-1.4	-0.9	-0.9	-0.2

Figure 2. A sample of the storm surge forecast message which is transmitted on Request/Reply twice each day. The storm surge height forecasts for Portland, Maine (PWM), Boston, Mass. (BOS), Newport, R.I. (NWP), Stamford, Conn. (SFD), Willets Point, N.Y. (LGA), New York, N.Y. (NYC), Atlantic City, N.J. (ACY), Breakwater Harbor, Del. (BWH), Baltimore, Md. (BAL), Norfolk, Va. (ORF), Avon, N.C. (AVN), and Charleston, S.C. (CHS) are made to 48 hours in advance at 6-h intervals. These forecasts, which are in feet, are based on sea-level pressure forecasts of the LFM model.

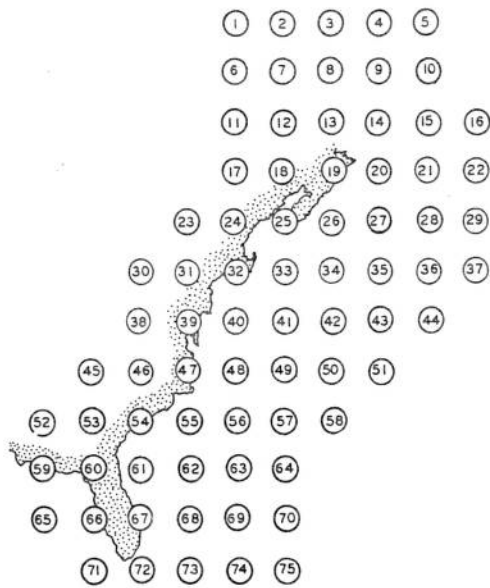


Figure 3. The location of the 75 NMC 6LPE grid points where analyzed sea-level pressures were available as predictors (from Pore et al., 1974).

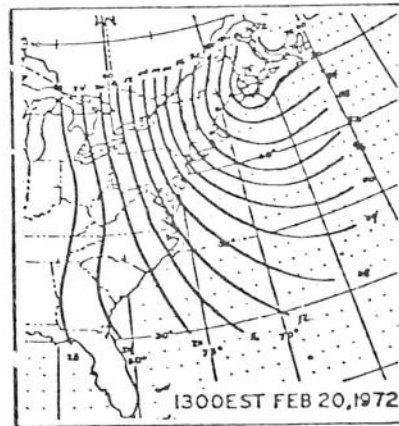
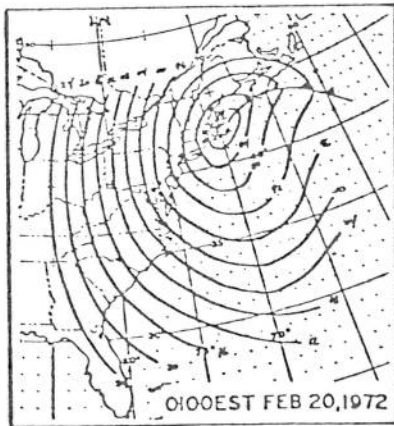
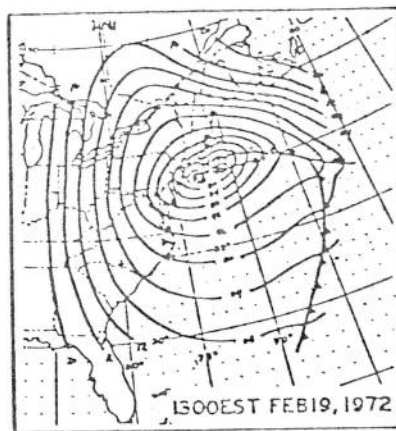
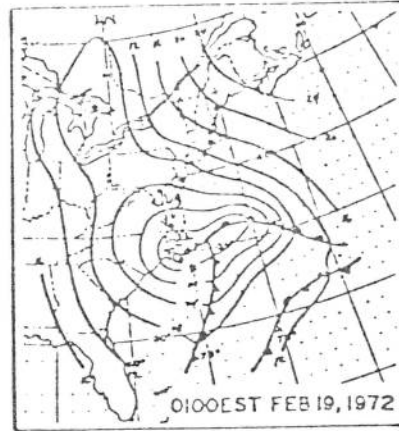
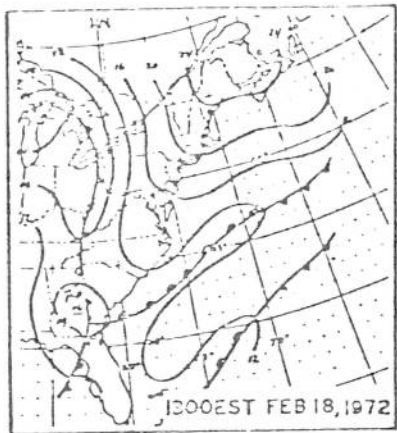


Figure 4. Sea-level pressure charts from 1300 EST February 18, 1972 to 1300 EST February 20, 1972.



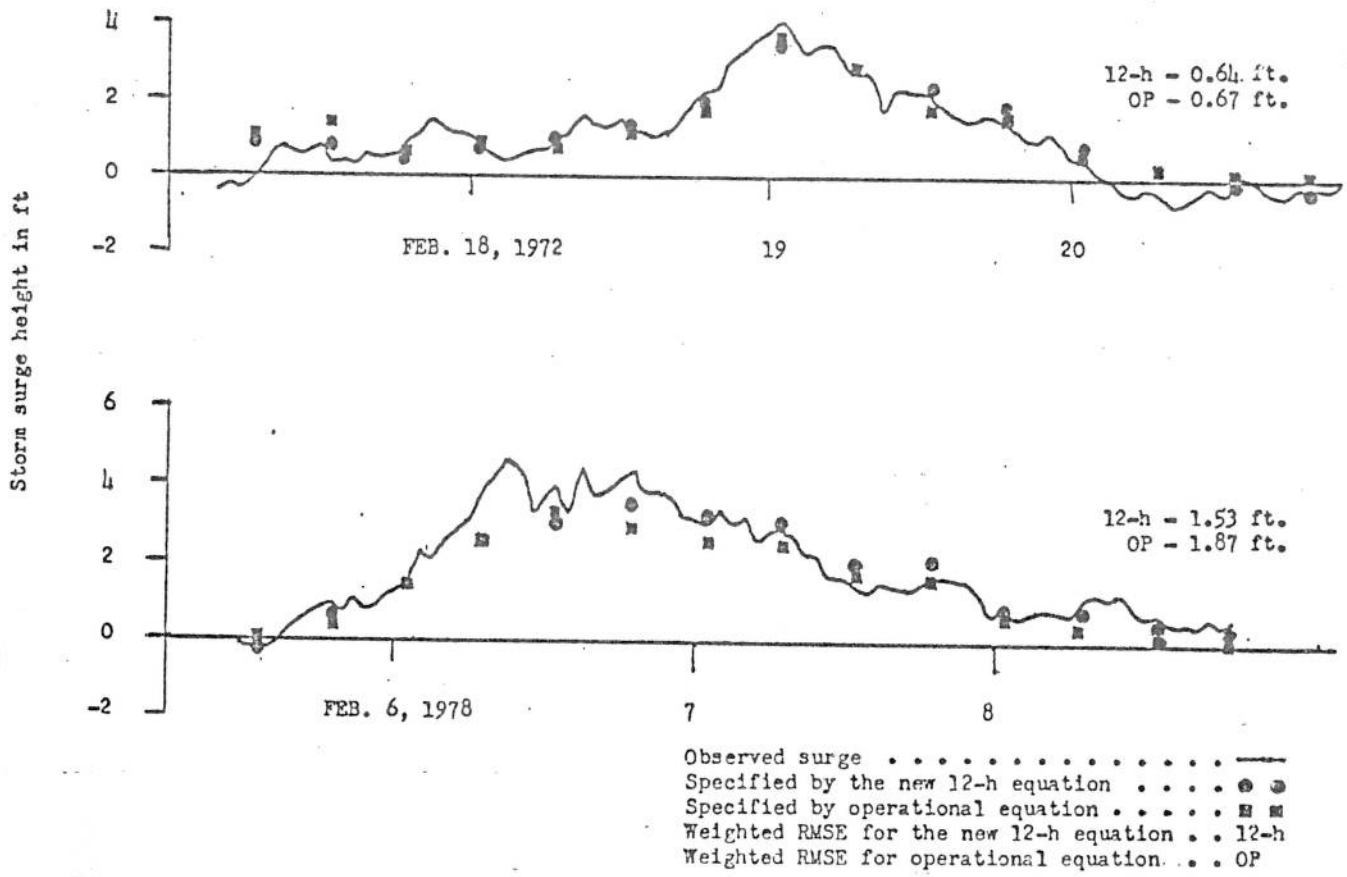


Figure 5. Two independent Boston storm surge events which occurred on February 18-20, 1972 (top graph) and February 6-8, 1978 (lower graph). Observed surges are shown as solid lines, while surges specified by the new 12-h equation and the operational equation are denoted by dots and squares, respectively. Coincident specifications are depicted by squares. Dates are placed at 1200 EST. Weighted RMSE's are given for the new 12-h equation and the operational equation from each event.

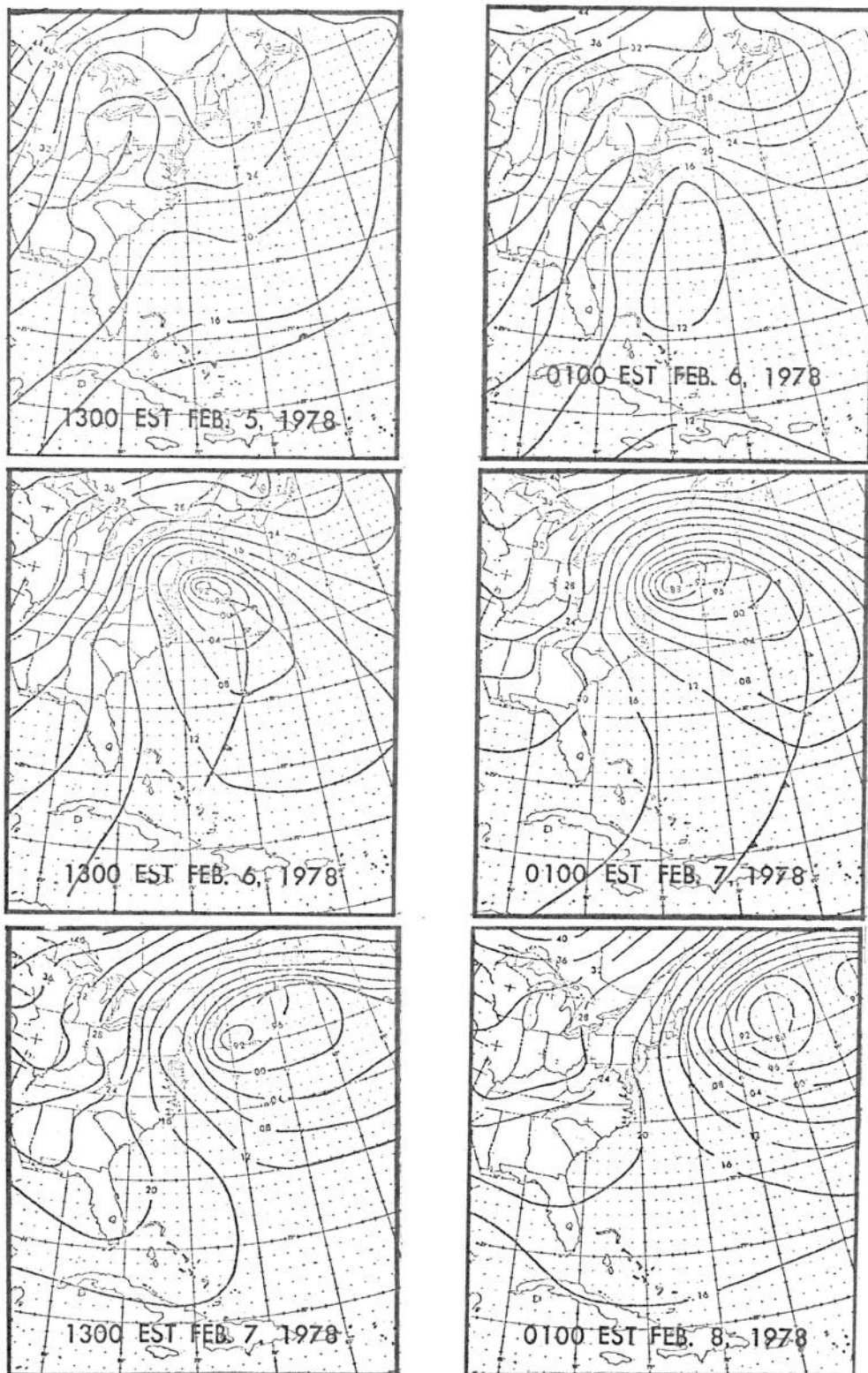


Figure 6. Sea-level pressure charts from 1300 EST February 5, 1978 to 0100 EST February 8, 1978.

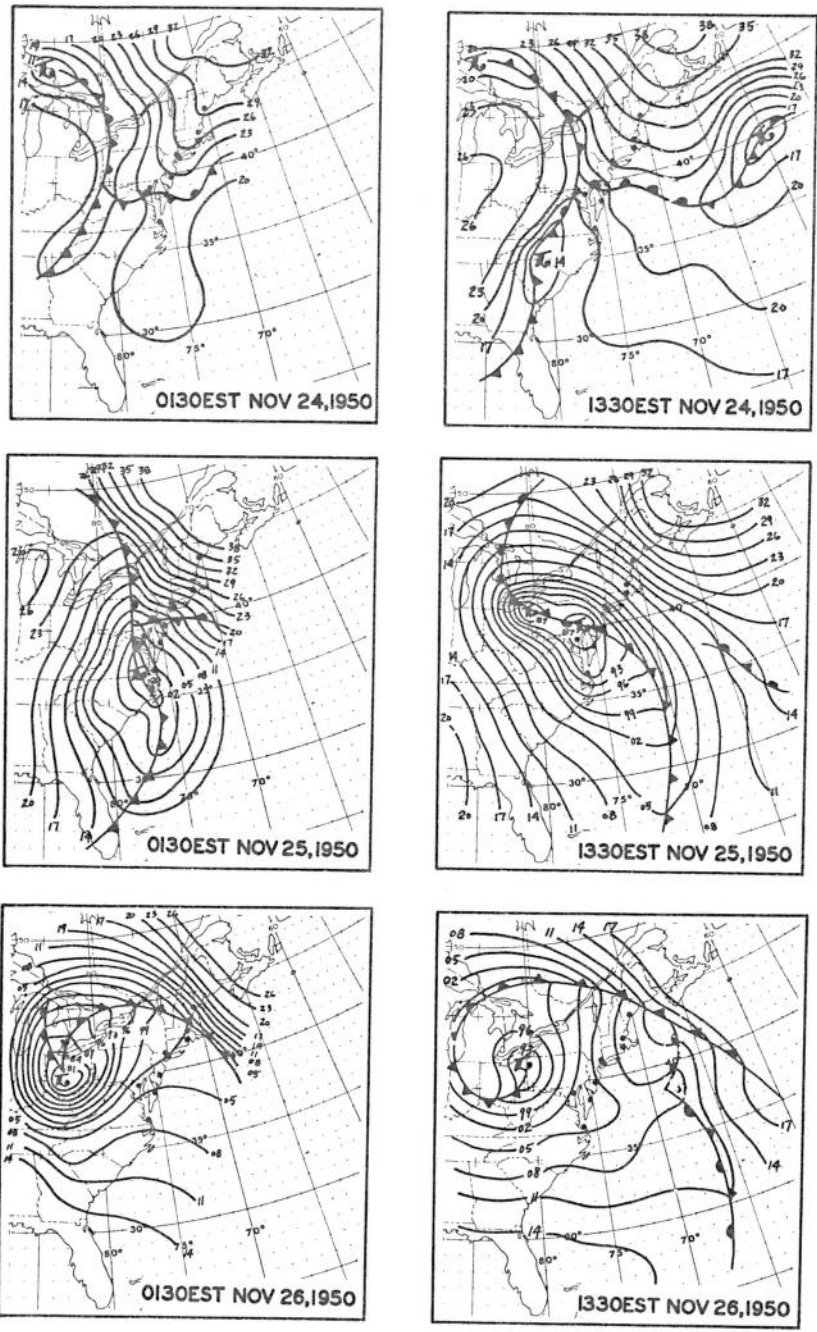


Figure 7. Sea-level pressure charts from 0130 EST November 24, 1950 to 1330 EST November 26, 1950.

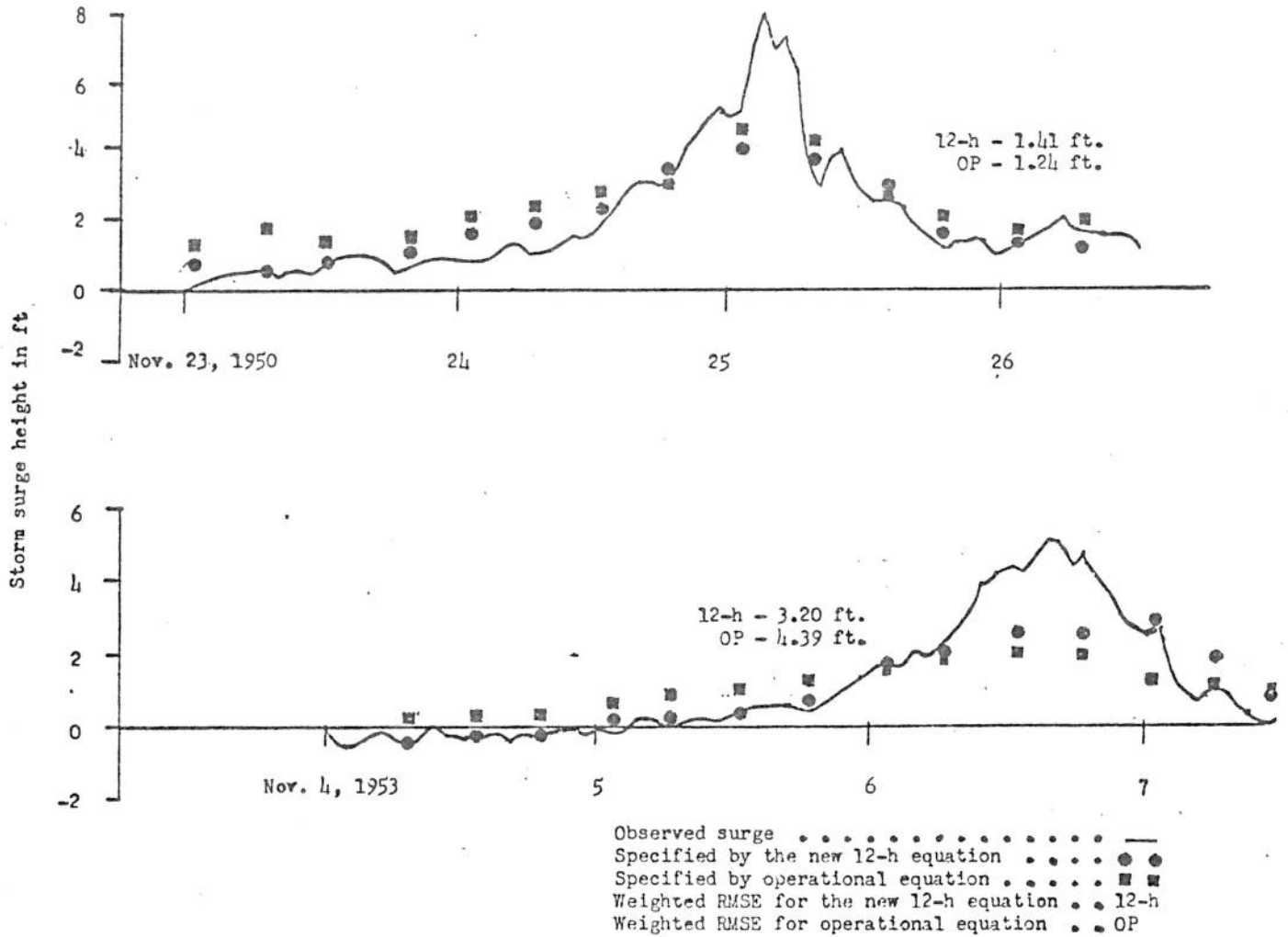


Figure 8. Same as Fig. 5 except for two New York events.

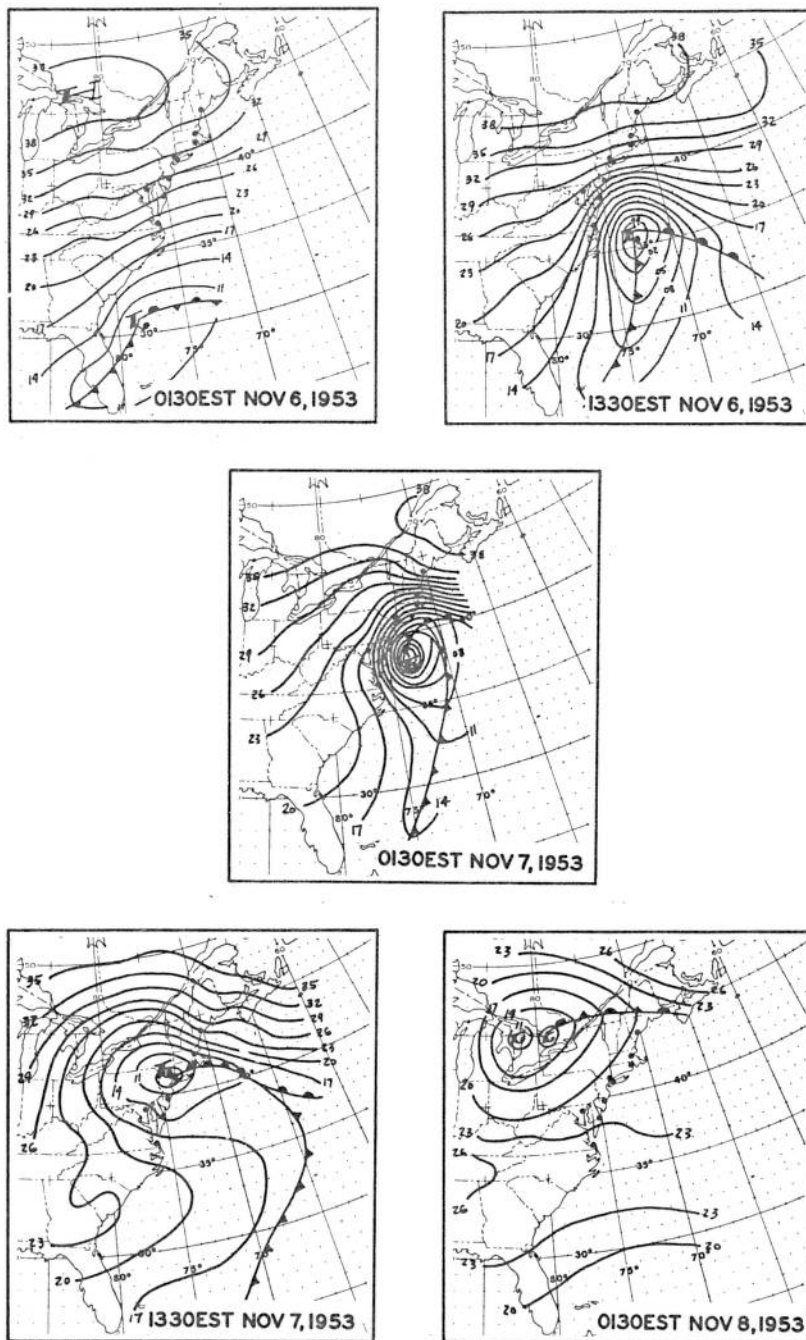


Figure 9. Sea-level pressure charts from 0130 EST November 6, 1953 to 0130 EST November 8, 1953.



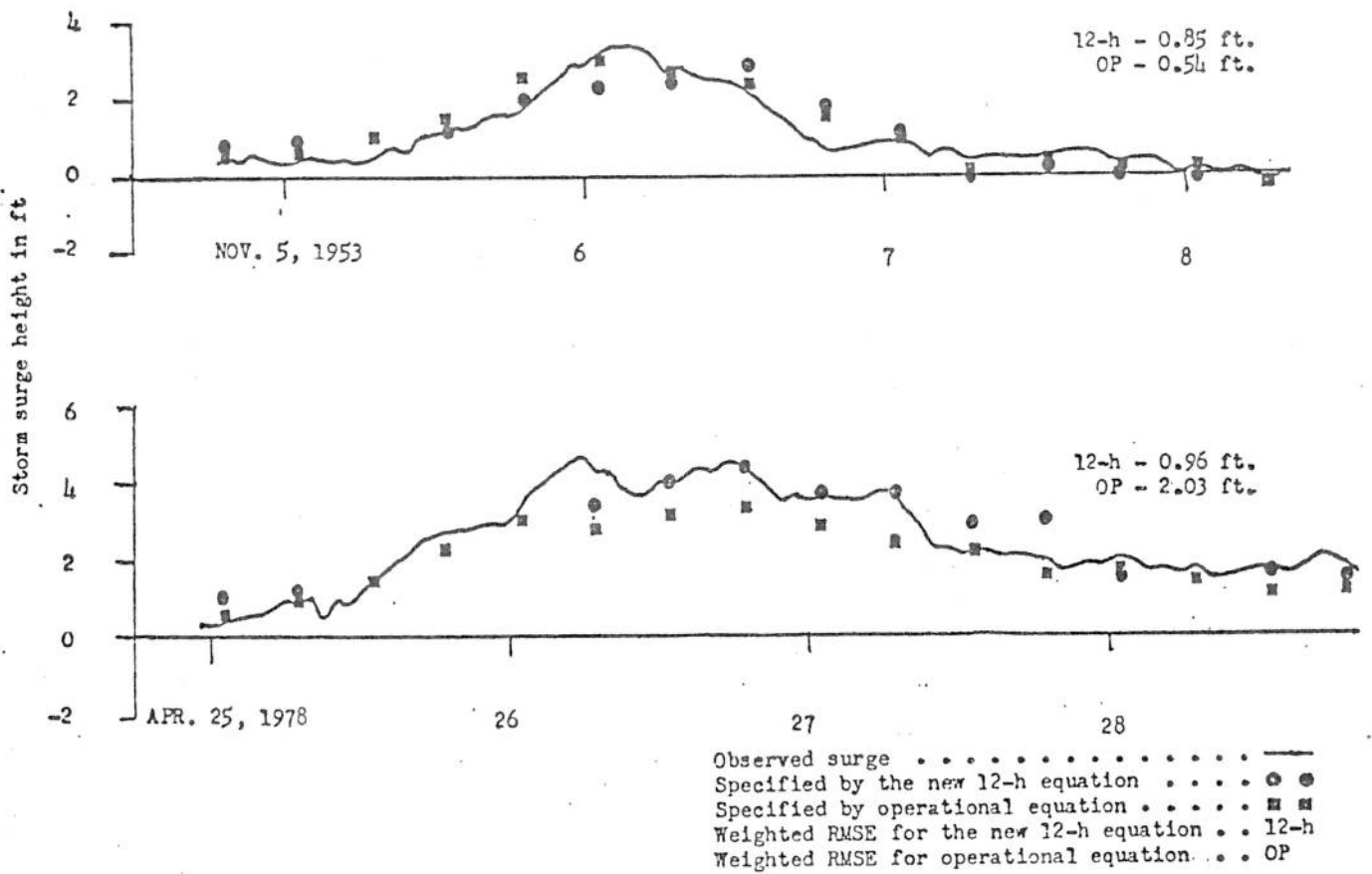


Figure 10. Same as Fig. 5 except for two Norfolk events.

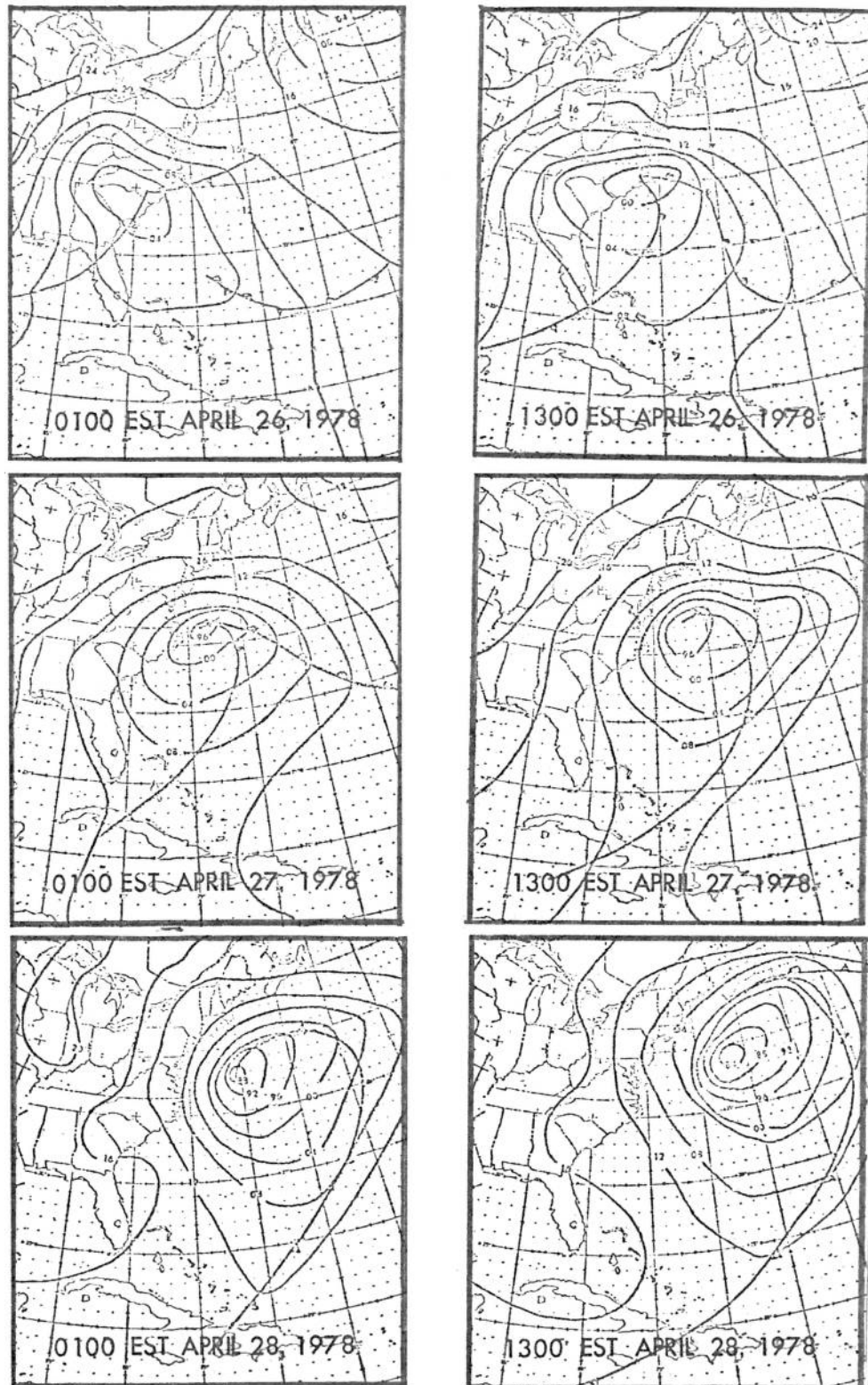


Figure 11. Sea-level pressure charts from 0100 EST April 26, 1978 to 1300 EST April 28, 1978.

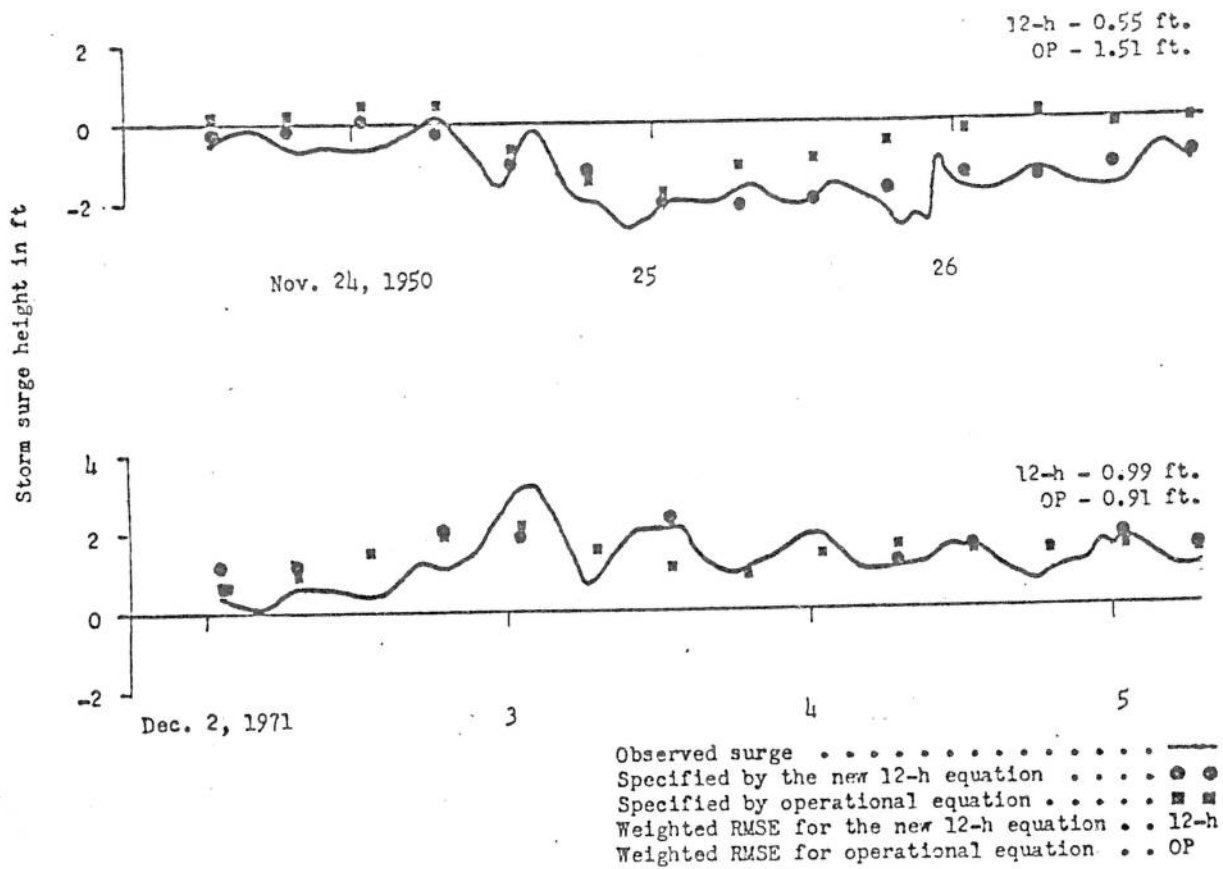


Figure 12. Same as Fig. 5 except for two Charleston events.

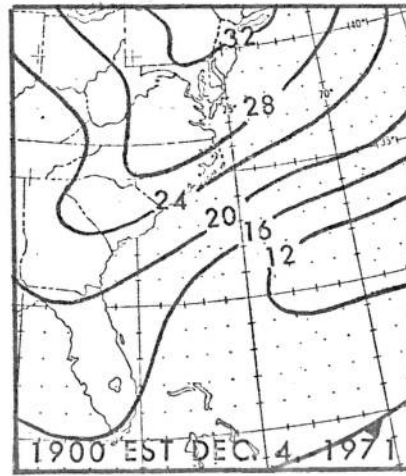
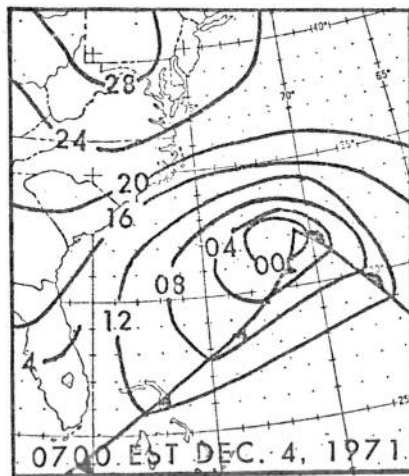
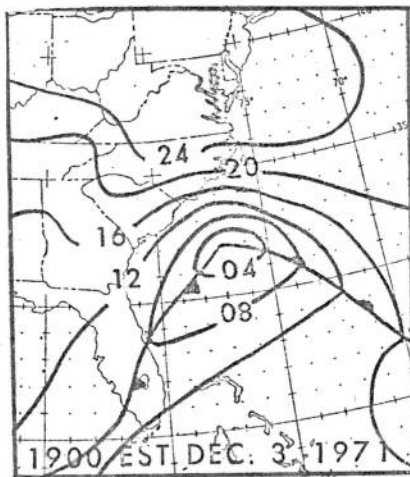
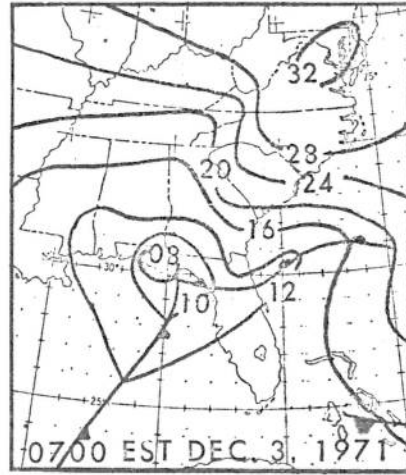
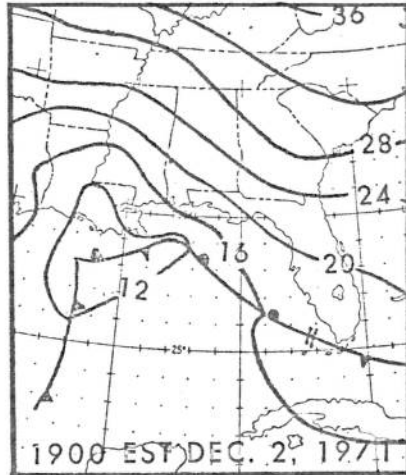


Figure 13. Sea-level pressure charts from 1900 EST December 2, 1971 to 1900 EST December 4, 1971.

Table 1. Dates of independent storm surge events which were used in the verification. Events used at each location are designated by the letter "X".

Dates of Independent Cases	Tide Gage Locations			
	Boston	New York	Norfolk	Charleston
Nov. 21-28, 1950	X	X	X	X
Nov. 3-8, 1953	X	X	X	X
Dec. 13-19, 1970	X	X	X	X
Dec. 1-7, 1971				X
Jan. 31-Feb. 6, 1972	X	X	X	
Feb. 15-21, 1972	X	X	X	
Nov. 6-9, 1974		X	X	X
Nov. 30-Dec. 4, 1974	X			
Mar. 12-21, 1975	X	X	X	X
Apr. 3-6, 1975	X	X	X	X
Apr. 15-17, 1975	X	X	X	X
Jan. 29-Feb. 3, 1976	X	X	X	X
Mar. 14-18, 1976	X	X	X	X
Feb. 5-11, 1978	X		X	X
Apr. 23-30, 1978		X	X	



Table 2. Verification scores associated with the new equations, persistence, and the operational equation for 12 independent Boston surge events. The new 12- and 24-h equations are denoted by BOS12 and BOS24. Six- and 12-h persistence are denoted by 6h and 12h. Scores tabulated in the top part of the table are based on all independent data (254 6-h heights). The lower part of the table shows the scores computed from peak data (37 6-h heights).

	New Equations		Persistence		Operational Equation
	BOS12	BOS24	6h	12h	
All Data					
Correlation coefficient	0.88	0.86	0.69	0.57	0.85
RMSE (feet)	0.50	0.53	0.80	0.94	0.55
WRMSE (feet)	0.90	0.98	1.58	2.02	0.99
Peak Data					
Correlation coefficient	0.94	0.94	0.69	0.50	0.93
RMSE (feet)	0.66	0.66	1.37	1.74	0.71
WRMSE (feet)	2.04	2.24	3.68	4.93	2.23

Table 3. Same as Table 2 except for 12 independent New York surge events. All data scores are based on 216 6-h heights, while scores associated with peak data were computed from 52 6-h heights. NYC06, NYC12, and NYC24 denote new 6-, 12-, and 24-h equations.

	New Equations			Persistence		Operational Equation
	NYC06	NYC12	NYC24	6h	12h	
All Data						
Correlation coefficient	0.92	0.89	0.85	0.84	0.59	0.81
RMSE (feet)	0.55	0.68	0.78	0.72	1.14	0.95
WRMSE (feet)	1.17	1.46	1.68	1.70	2.69	1.95
Peak Data						
Correlation coefficient	0.96	0.95	0.93	0.88	0.68	0.90
RMSE (feet)	0.73	0.91	1.09	1.09	1.72	1.26
WRMSE (feet)	2.22	2.79	3.20	3.31	5.24	3.67

Table 4. Same as Table 2 except for 13 independent Norfolk surge events.

All data scores are based on 224 6-h heights while scores associated with peak data were computed from 53 6-h heights. ORF06, ORF12, ORF18, and ORF24 denote the 6-, 12-, 18-, and 24-h equations.

	New Equations				Persistence		Operational Equation
	ORF06	ORF12	ORF18	ORF24	6h	12h	
All Data							
Correlation coefficient	0.92	0.91	0.89	0.86	0.88	0.78	0.80
RMSE (feet)	0.40	0.42	0.46	0.50	0.49	0.66	0.61
WRMSE (feet)	0.54	0.56	0.65	0.89	0.74	1.13	0.92
Peak Data							
Correlation coefficient	0.95	0.94	0.93	0.90	0.91	0.79	0.87
RMSE (feet)	0.36	0.40	0.45	0.56	0.54	0.84	0.64
WRMSE (feet)	0.92	0.97	1.17	1.69	1.37	2.19	1.67

Table 5. Same as Table 2 except for 11 independent Charleston surge events. All data scores are based on 203 6-h heights while scores associated with peak data were computed from 17 6-h heights. CHS06, CHS12, and CHS24 denote the new 6-, 12-, and 24-h equations.

	New Equations			Persistence		Operational Equation
	CHS06	CHS12	CHS24	6h	12h	
All Data						
Correlation coefficient	0.81	0.86	0.79	0.72	0.73	0.66
RMSE (feet)	0.47	0.43	0.50	0.59	0.58	0.63
WRMSE (feet)	0.56	0.46	0.55	0.72	0.91	0.67
Peak Data						
Correlation coefficient	0.95	0.96	0.94	0.92	0.75	0.92
RMSE (feet)	0.76	0.58	0.78	0.85	1.28	1.00
WRMSE (feet)	1.67	1.30	1.61	1.97	2.95	1.91

APPENDIX

NEW EQUATIONS FOR BOSTON, NEW YORK, NORFOLK, AND CHARLESTON

$$\begin{aligned}
 \text{BOS12}_T &= 34.09 + 0.00367 \text{ GP}(41)_T + 0.00191 \text{ GP}(12)_T \\
 &\quad - 0.05514 \text{ GP}(33)_T - 0.01042 \text{ GP}(16)_T \\
 &\quad + 0.3198 \text{ SS}_{T-12} + 0.05446 \text{ GP}(18)_T \\
 &\quad - 0.02792 \text{ GP}(32)_T \\
 \\
 \text{BOS24}_T &= 42.87 + 0.00829 \text{ GP}(41)_T + 0.01202 \text{ GP}(12)_T \\
 &\quad - 0.03652 \text{ GP}(33)_T - 0.0089 \text{ GP}(16)_T \\
 &\quad + 0.165 \text{ SS}_{T-24} + 0.05044 \text{ GP}(18)_T \\
 &\quad - 0.04222 \text{ GP}(32)_T - 0.02517 \text{ GP}(34)_T \\
 \\
 \text{NYC06}_T &= 22.55 + 0.54141 \text{ SS}_{T-6} + 0.06343 \text{ GP}(24)_{T-6} \\
 &\quad - 0.05742 \text{ GP}(39)_T - 0.02789 \text{ GP}(42)_{T-12} \\
 \\
 \text{NYC12}_T &= 23.37 - 0.03714 \text{ GP}(47)_{T-6} - 0.00849 \text{ GP}(17)_{T-6} \\
 &\quad + 0.3454 \text{ SS}_{T-12} - 0.08797 \text{ GP}(39)_T \\
 &\quad - 0.01886 \text{ GP}(42)_{T-18} + 0.09623 \text{ GP}(24)_{T-6} \\
 &\quad + 0.05567 \text{ GP}(47)_T - 0.02194 \text{ GP}(42)_T \\
 \\
 \text{NYC24}_T &= 24.19 - 0.0065 \text{ GP}(47)_{T-6} - 0.00033 \text{ GP}(17)_{T-6} \\
 &\quad - 0.0174 \text{ GP}(42)_{T-18} - 0.05732 \text{ GP}(39)_{T-6} \\
 &\quad + 0.10704 \text{ GP}(24)_{T-6} + 0.24602 \text{ SS}_{T-24} \\
 &\quad - 0.026 \text{ GP}(42)_T - 0.06484 \text{ GP}(39)_T \\
 &\quad + 0.04214 \text{ GP}(47)_T \\
 \\
 \text{ORF06}_T &= 8.80 + 0.82341 \text{ SS}_{T-6} - 0.00566 \text{ GP}(24)_T \\
 &\quad - 0.0514 \text{ GP}(47)_T + 0.04852 \text{ GP}(31)_T \\
 \\
 \text{ORF12}_T &= 15.16 + 0.7456 \text{ SS}_{T-12} - 0.00284 \text{ GP}(17)_T \\
 &\quad + 0.00442 \text{ GP}(55)_T + 0.0687 \text{ GP}(31)_T \\
 &\quad - 0.08504 \text{ GP}(47)_T \\
 \\
 \text{ORF18}_T &= 19.52 + 0.6165 \text{ SS}_{T-18} + 0.00807 \text{ GP}(17)_{T-6} \\
 &\quad + 0.00243 \text{ GP}(55)_T + 0.08118 \text{ GP}(31)_T \\
 &\quad - 0.0634 \text{ GP}(47)_T - 0.04723 \text{ GP}(47)_{T-6} \\
 \\
 \text{ORF24}_T &= 39.11 + 0.03909 \text{ GP}(17)_{T-18} - 0.00998 \text{ GP}(55)_{T-6} \\
 &\quad + 0.39483 \text{ SS}_{T-24} + 0.01430 \text{ GP}(24)_T \\
 &\quad - 0.02472 \text{ GP}(42)_{T-18} - 0.02065 \text{ GP}(6)_T \\
 &\quad - 0.05149 \text{ GP}(47)_T + 0.07203 \text{ GP}(31)_T \\
 &\quad - 0.05679 \text{ GP}(47)_{T-6} \\
 \\
 \text{CHS06}_T &= 47.31 + 0.18646 \text{ SS}_{T-6} + 0.05178 \text{ GP}(39)_T \\
 &\quad - 0.06249 \text{ GP}(60)_T - 0.03558 \text{ GP}(58)_{T-12} \\
 &\quad + 0.2704 \text{ SS}_{T-12} \\
 \\
 \text{CHS12}_T &= 22.22 + 0.00155 \text{ GP}(39)_{T-6} + 0.4994 \text{ SS}_{T-12} \\
 &\quad - 0.02373 \text{ GP}(42)_{T-6} - 0.08028 \text{ GP}(60)_T \\
 &\quad + 0.08075 \text{ GP}(46)_{T-6}
 \end{aligned}$$

$$\begin{aligned}
\text{CHS24}_T &= 59.83 + 0.02529 \text{ GP}(39)_{T-6} - 0.08082 \text{ GP}(60)_T \\
&\quad - 0.04567 \text{ GP}(58)_{T-12} + 0.3135 \text{ SS}_{T-24} \\
&\quad + 0.0426 \text{ GP}(39)_T
\end{aligned}$$

The term to the left of the equal sign is the storm surge forecast in feet at verifying time T. The three left most characters of this term designate gage location BOS (Boston), NYC (New York), ORF (Norfolk), and CHS (Charleston). The number following the locations designator is the lag time in hours of the storm surge predictor. GP is the sea-level pressure in millibars at the indicated grid point (see Fig. 3). SS is the storm surge height in feet. The negative numbers of the pressure and surge subscripts are time lags in hours.